JTTEE5 11:179-185

Scaling Analysis and Prediction of Thermal Aspects of the Plasma Spraying Process Using a Discrete Particle Approach

Jinho Lee and Theodore L. Bergman

(Submitted 28 July 2001)

On the basis of a discrete particle approach, a scaling analysis was used to predict features of the thermal plasma spraying process. Correlations were obtained using the analysis and they were subsequently used to predict two important features: the state of the particle at the moment of impact on the substrate, and the nature of solidification process. Limitations and restrictions were also identified in the development of the analysis that can be used to infer the resulting structure of coating. The correlations that were developed might be utilized in optimizing the thermal plasma spraying process, as well as in producing new types of coatings.

Keywords discrete particle event, product quality prediction, scaling analysis

1. Introduction

Thermal plasma spraying has become an important technology for the production of thermal barriers, as well as corrosion-, wear-, and erosion-resistant coatings. Principle areas of current research related to this process can be categorized as (1) plasma fluid flow and thermal characterization, (2) investigation of particle entrainment and heat transfer in the plasma, and (3) description of the solidification of the sprayed material and the associated development of the coating microstructure.

Individual aspects of problems related to each of the preceding issues have been studied extensively and are well documented in the literature.[1-3] For industrial applications, for which a higher quality coating or improved manufacturing efficiency is desired, these and many other works have yet to be synthesized into a comprehensive model. Furthermore, when an experimental approach is taken, it is impossible to study the entire process comprehensively because of the great number of variables and parameters involved. Usually, a prohibitively large number of experiments would be needed to scrutinize the entire process. Alternatively, numerical work has been done to overcome this dilemma and has enjoyed limited success; however, direct simulation of the entire process would be intolerably time consuming. Thus, there remains a need to predict, a priori, the quality of the final coating in terms of basic operating variables. In this study, an attempt is made using scaling analysis to establish correlations that link the process characteristics and basic operating parameters in the thermal plasma spraying process to the quality of final product. The scaling analysis considers the deposition of discrete particles.

Jinho Lee, Department of Mechanical Engineering, Yonsei University, Seoul, 120-749, Korea; and **Theodore L. Bergman,** Department of Mechanical Engineering, University of Connecticut, Storrs, Connecticut 06269-3139. Contact e-mail: theodore.bergman@uconn.edu.

2. Scaling Analysis

Typically, the sprayed particles are fully molten during their flight and will impinge on the substrate surface with a sufficiently high velocity to promote high deposition efficiencies. Thus, upon impact and subsequent deformation and solidification, a fully coherent and potentially nonporous coating may be produced. Alternatively, when production of thermal barrier coatings is required, partially molten impacting particles may be preferred in order to produce some porosity in the coating. Therefore, the prediction of the particle state at the time of impact is important to predict the subsequent solidification process and coating quality.

The present work consists of two parts: prediction of the particle state at the moment of impingement upon the substrate (or existing coating), and prediction of the solidification process. An analysis is made of a single particle's behavior by considering the average value of the addition of a splat to the top surface of the previously deposited surface. The summation of many such events yields a deposit consisting of a series of layered splats. In the following discussion, a scaling analysis of the particle state at the moment of impact is developed, and is followed by a scaling analysis of the solidification process.

2.1. Prediction of the Particle State at Impact

Figure 1 shows a schematic diagram associated with the present study. It is assumed that the spray from the plasma torch nozzle is conical in shape, and consists of a random distribution of mono-size particles of average diameter, d_p. The spray is in a quasi-steady state because it is assumed that neither the plasma torch nor substrate moves with respect to the other, and that the particle is heated isothermally (that is, it has negligibly small internal temperature gradients) while traveling in the plasma gas. The last assumption is justified when the Biot number, which is based upon the particle diameter, is much less than unity; i.e., for $Bi = h_g d_p/k << 1$, where h_g is the heat transfer coefficient of the plasma gas surrounding the particle, and k is

Nomenclature

A_s	particle surface area, m^2
A_{sub}	particle deposition area, m^2
A_ξ	splat area, m^2
c	specific heat, J/kg · K
d_p	particle diameter, m
d_s	equivalent diameter, m
D	splat diameter, m
f_s	solid fraction
h_g	convective heat transfer coefficient of plasma gas, $W/m^2 \cdot K$
h_s	contact heat transfer coefficient to the substrate, $W/m^2 \cdot K$
H	deposit thickness, m
H_{sf}	latent heat of melting, J/kg
H_p	energy to be removed for solidification, J
k	thermal conductivity, W/m · K
L	torch standoff distance, m
L_s	location at the onset of particle melting, m
L_f	location of complete particle melting, m = $L_s + L_{sf}$
L_{sf}	distance traveled by particle during melting, m
l_t	thickness of solidified layer, m
$\dot{M}$	mass flow rate of particle, kg/s
$\dot{N}$	particle deposition rate, s^{-1}
$\dot{Q}_{conv}$	convection rate from plasma gas, W
$\dot{Q}_{sub}$	heat extraction rate through substrate, W
q_{conv}	convection heat flux from plasma gas, W/m^2
q_{sub}	heat extraction flux through substrate, W/m^2
R_{cond}	internal conduction resistance of deposit, K/W
S_t	splat thickness, m
T	temperature, K
ΔT_s	degree of superheat, K
t	time, s
t_{fr}	particle solidification time scale, s
t_l	liquid layer formation time
t_{sa}	subsequent particle arriving time scale, s
t_{sp}	particle spreading time scale, s
u_p	particle velocity, m/s
V	particle volume, m^3
x	axial coordinate, m
Bi	biot number based on particle diameter = $h_g d_p/k$
Bi_s	biot number based on splat thickness = $h_s S_t/k$
ξ	spread factor = D/d_p
ρ	particle density, kg/m^3
τ_{fv}	time taken to reach evaporating temperature, s
τ_s	time to reach melting point, s

Subscripts

evp	evaporation
g	plasma gas
go	plasma gas at torch nozzle exit
i	impact
m	melting
p	particle
po	particle at torch exit

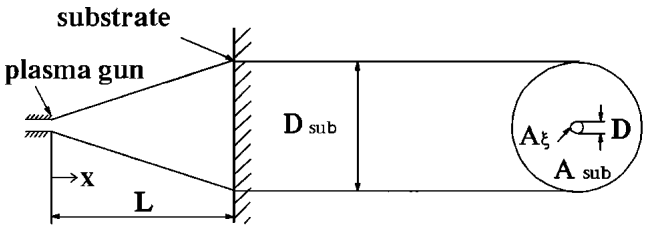

Fig. 1 Schematic diagrams of the present study: **(a)** physical system, **(b)** deposition circle and single splat (amplified)

the particle's thermal conductivity. Note that the particle isothermality assumption becomes suspect for ceramic particles with $Bi \sim 1$. Both h_g and k vary during particle translation in the plasma, and if the variation becomes large, properly averaged values should be used.

The particle's state can be determined in terms of the distance between the plasma torch nozzle and the substrate distance, L. One may consider the location where the particle begins to melt, L_s, and where particle completes its melting, L_f. These locations can be found from an energy balance applied to the particle:

$$\text{during heating: } -\rho c V \frac{dT_p}{dt} = h_g A_s (T_p - T_g) \quad \text{(Eq 1)}$$

$$\text{during melting: } \rho V H_{sf} \frac{df_s}{dt} = h_g A_s (T_m - T_g) \quad \text{(Eq 2)}$$

where ρ, V, c, A_s, and H_{sf} are the particle's density, volume, specific heat, surface area, and latent heat of melting, respectively. The variables T_p, T_m, and T_g are the instantaneous particle temperature, the material (particle) melting temperature, and the plasma gas temperature, respectively, whereas f_s and t are the particle's solid fraction and time, respectively. By separation of variables, Eq 1 can be rewritten as:

$$\int \frac{dT_p}{T_p - T_g} = -\int_0^t \frac{hA_s}{\rho V c}\, dt \quad \text{(Eq 3)}$$

Numerical and experimental results show that for most of the heating period, the particle temperature increases very rapidly, reaching its melting point in regions of the plasma jet where the plasma temperature varies rather slowly.[4-7] Thus during this period $dT_p >> dT_g$ and

$$dT_p \approx d(T_p - T_g) \quad \text{(Eq 4)}$$

Available numerical results also show that, in many cases, the plasma temperature at the melting position, $T_{g|x=Ls}$, does not differ greatly from its initial temperature, T_{go}.[4-6] Then, from the combination of Eq 3 with Eq 4, the duration of time, τ_s, taken for the particle to reach its melting point, T_m, can be expressed as

$$\tau_s = \frac{\rho V \bar{c}}{\bar{h} A_s} \ln \frac{T_{go} - T_{po}}{T_{go} - T_m} \quad \text{(Eq 5)}$$

where T_{go} and T_{po} are plasma and particle's initial temperatures, i.e., at the plasma torch nozzle exit and $\bar{h}$ and $\bar{c}$ are average values of h_g and c during time τ_s. When the plasma temperature

decreases rapidly, the temperature T_{go} needs to be replaced by $T_g|_{x=L_s}$.[7] Possible resolidification in flight is not accounted for because this situation is, in general, undesirable.

Denoting the distance from nozzle exit at which particle starts to melt as L_s, and also denoting the distance traveled beyond L_s until the particle is completely melted as L_{sf}, the total distance from torch nozzle to where particle completes melting, L_f, is

$$L_f = L_s + L_{sf} \quad \text{(Eq 6)}$$

When the substrate is located between L_s and L_f, the particle arrives at the substrate in a partially molten state and its solid fraction is given from integration of Eq 2 as

$$1 - f_s = \frac{\bar{h}A_s\,\overline{(T_g - T_m)}}{\rho V H_{sf}} \cdot \frac{L - L_s}{\overline{u_p}} \quad \text{(Eq 7)}$$

where $\overline{u_p}$ is the average particle velocity. Alternatively, when the substrate is located at L_f, the particle arrives in a fully molten state, and when the substrate is located beyond L_f, the particle would be either superheated (if heating continues) or in a resolidified state if cooling occurs. In the case when the plasma temperature is larger than the particle melting temperature, the particle will be overheated and the degree of superheating, ΔT_s can be approximated as

$$\Delta T_s = \frac{\bar{h}A_s\,\overline{(T_g - T_p)}}{\rho V \bar{c}} \cdot \frac{L - L_f}{\overline{u_p}} \quad \text{(Eq 8)}$$

where $\Delta T_s = T_p - T_m$, $\overline{(T_g - T_p)}$ is the average temperature difference between the plasma and the particle temperature and $[(L - L_f)/\overline{u_p}]$ is the duration of time during superheating. The time, τ_{fv}, when the particle reaches its evaporation temperature, T_{evp}, is derived from Eq 8 and is

$$\tau_{fv} = \frac{\rho V \bar{c}(T_{evp} - T_m)}{\bar{h}A_s\,\overline{(T_g - T_p)}} \quad \text{(Eq 9)}$$

The distance traveled by the particle during this period is

$$L_{fv} = \tau_{fv}\,\overline{u_p} \quad \text{(Eq 10)}$$

Evaporation reduces the particle size at impact, and causes an increase of porosity in the deposit, and thus should be avoided if high-density coatings are preferred.[8,9]

Summarizing the above results in terms of basic parameters, the particle state at the moment of impact is given in Table 1. The results reported in Table 1 are meaningful in that they show the important parameters explicitly, and how they are related. The usefulness of the results, however, largely depends on how accurately one can determine $\overline{u_p}$, $\overline{(T_g - T_p)}$, and $\bar{h}$. Estimates of the values of these parameters could be obtained from available experimental or numerical results.

For the superheated particle state, the results of Table 1 can be used to estimate whether the particle goes to a superheated state when the plasma temperature is larger than particle's melting temperature. However, the degree of superheat may only be determined through the knowledge of particle temperature variation.

Table 1 The State of Particle at the Moment of Impact upon the Substrate

Physical Condition	Particle Size
$\frac{L}{\overline{u_p}} \le \frac{\rho V \bar{c}}{\bar{h}A_s} \ln \frac{T_{go} - T_{po}}{T_{go} - T_m}$	Solid state
$\frac{\rho V \bar{c}}{\bar{h}A_s} \ln \frac{T_{go} - T_{po}}{T_{go} - T_m} < \frac{L}{\overline{u_p}} \le \frac{\rho V H_{sf}}{\bar{h}A_s(T_g - T_m)}$	Partially or fully molten state
$\frac{\rho V H_{sf}}{\bar{h}A_s(T_g - T_m)} < \frac{L}{\overline{u_{p,i}}} \le \frac{\rho V c(T_{evp} - T_m)}{\bar{h}A_s(T_g - T_p)}$	Superheated state

2.2. Time Scales of the Solidification Process

The quality of the coating or deposit during thermal plasma spraying largely depends on the solidification process after the particles impact upon the relatively cold substrate. From the discrete event point of view, the coating is built up particle by particle and no splashing is assumed to occur. Particles reach the substrate in a partially or fully molten state, or in a superheated state. They spread quickly to form splats and subsequently cool and solidify. Subsequent particles arrive at the same (or nearby) spot after some time interval. The spreading time varies depending on the arriving particle's state and velocity. In addition, the solidification time varies depending on the heat extraction rate from substrate and the heat supply from the hot plasma gas. Finally, the splat formed from the initial particle either solidifies completely or only partially solidifies before the arrival of the subsequent particle, depending on the time interval associated with the arrival of the next splat. In the former case (where the splat completes solidification before next particle arrives), the following splat may undergo a different solidification rate because of the presence of a thermal contact resistance between the molten (second) splat and the solidified (first) splat. In the case where each splat solidifies before the arrival of a subsequent particle, the coating deposit consists of an agglomeration of splats, which is known to offer fine grain structure, but the grains may be columnar and the porosity level may be too high for a specific purpose. If, however, each splat does not complete solidification, a liquid layer will exist on top of each splat, which acts to reduce porosity.[1,2]

On the basis of the above observations, the solidification process may be broken into four distinct time scales. The splat is assumed to be a thin circular disk of diameter D and thickness S_t. The deposition efficiency is assumed to be unity.

2.2.1 Splat Spreading Time Scale, t_{sp}. The deformation (flattening and spreading) of a molten particle on a substrate after impact has been studied extensively, and models for the extent of spreading, described in terms of a dimensionless diameter, $\xi = D/d_p$, have been proposed and examined.[1-14] On the basis of these models, the spreading time scale can be roughly estimated by considering the time needed to fill a shallow, cylindrical volume by an impinging molten particle.

Considering the molten particle's volume flow as an equivalent cylindrical volumetric flow of diameter d_s and height equal to the particle's diameter d_p, with impinging velocity $u_{p,i}$ (Fig. 2), the spreading time scale, t_{sp}, is

$$\frac{\pi}{4} d_s^2 u_{p,i} t_{sp} = \frac{\pi}{4} D^2 S_t \quad \text{(Eq 11)}$$

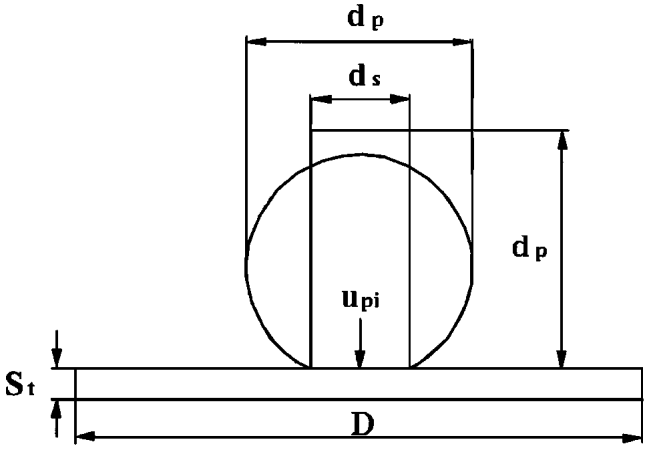

Fig. 2 Model of particle spreading

From conservation of mass, it may be shown that

$$d_t = \sqrt{\frac{2}{3}} d_p \qquad \text{(Eq 12)}$$

Then, from Eq 11 and 12 it follows that

$$t_{sp} = \frac{3}{2}\xi^2 \frac{S_i}{u_{p,i}} = \frac{d_p}{u_{p,i}} \qquad \text{(Eq 13)}$$

Fukanuma[15] analytically obtained the time for the splat to spread to 90% of its maximum diameter, D_m, as

$$t_{0.9} = 0.479 \frac{d_p}{u_{p,i}} \cdot \frac{D_m}{d_p} \qquad \text{(Eq 14)}$$

Considering its approximate nature and noting that D_m/d_p usually takes a value of 2 to 4, the present estimate for the spreading time agrees well with Fukanuma's relation. For d_p = 10^{-5} m and $u_{p,i}$ = 100 m/s, the spreading time from Eq 13 is on the order of 10^{-7} s, which is in good agreement with the numerical result obtained by Liu et al.[16]

In deriving Eq 13, it is assumed that the particle reaches the substrate in a fully molten state, which is conventionally the case in thermal plasma spraying. For a partially molten particle (unless the solid fraction is large) partial solidification does not affect the spreading significantly, because of the importance of the kinetic energy, thus Eq 13 still can be used to estimate the spreading time.[17] Molten particles with high solid fractions are not considered here. The effects of surface roughness, droplet-substrate wetting, and other local effects are not considered here.

2.2.2 Time Scale Between Particle Arrivals, t_{sa}. The time interval between two successive particles arriving at the substrate can be estimated using the rate of particle deposition, $\dot{N}$, or particle mass flow rate, $\dot{M}$, *as*

$$t_{sa} = \frac{1}{\dot{N}} \frac{A_\xi}{A_{sub}} = \frac{\frac{\pi}{6}\rho d_p^3}{\dot{M}} \frac{A_\xi}{A_{sub}} \qquad \text{(Eq 15)}$$

where A_ξ is the area of a single splat, and A_{sub} can be determined experimentally or can be approximated from turbulent jet theory.[18]

2.2.3 Solidification Time Scale, t_{fr}. The solidification time scale, t_{fr}, associated with the completion of solidification of a single molten particle after impacting the substrate can be estimated from a simple energy balance for a pure material as

$$t_{fr} = \frac{H_p}{\dot{Q}_{sub} - \dot{Q}_{conv}} \qquad \text{(Eq 16)}$$

where H_p is the amount of heat to be removed from a molten particle for complete solidification, $\dot{Q}_{sub}$ is the rate of heat extraction through substrate and $\dot{Q}_{conv}$ is the convective heat transfer from the plasma gas to a solidifying particle until a subsequent particle arrives. Radiation heat transfer is assumed to be negligibly small. Expressions for the heat transfer rates are

$$H_p = \rho V(1 - f_s)H_{sf} \quad \text{for a molten particle} \qquad \text{(Eq 17a)}$$

$$\text{or} \quad H_p = \rho V H_{sf} + \rho c V T_s \quad \text{for a superheated particle} \qquad \text{(Eq 17b)}$$

$$\text{and} \quad \dot{Q}_{sub} = h_s A_\xi \overline{(T_p - T_s)_i} \qquad \text{(Eq 18)}$$

$$\dot{Q}_{sub} = h_s A_\xi (T_g - T_p)_i \qquad \text{(Eq 19)}$$

In these expressions, h_s is the interfacial heat transfer coefficient between the splat and the substrate, whereas h_g is the plasma gas convective heat transfer coefficient. The expression $\overline{(T_p - T_s)_i}$ is the average temperature difference between particle temperature at the moment of impact and the substrate temperature.

The particle temperature at the time of impact is, at minimum, its melting temperature. The subscript i denotes the impact state.

2.3. Single Splat Prediction

Because it is assumed that the solidification of an individual particle is not affected by other particles, the property of a coating can be regarded as an ensemble result of the spreading and solidification of many individual particles.[19] By comparing relative magnitudes of the time scale related to the relevant process over a single particle, reasonable predictions of the solidification process can be made.

2.3.1 Effect of Solidification on Spreading

(i) $t_{fr} >> t_{sp}$

Usually, the particle size is very small, on the order of 10 μm, and the impact velocity is on the order of 10^2 m/s. Thus, from Eq 13 , the spreading time scale, t_{sp}, is on the order of 10^{-7} s, which is much less than the usual solidification time scale, which is on the order of 10^{-3} to 10^{-5} s. In general, in thermal plasma spraying the kinetics of the particle spreading exceeds that of solidification by two orders of magnitude.[20] When the spreading time scale is significantly less than the solidification time scale, the particle completes spreading to its maximum extent prior to the initiation of solidification.

(ii) $t_{fr} \geq t_{sp}$

When the particle size is relatively large, on the order of 10^2-10^3 μm, and the impact velocity is relatively small, on the order of 1-10 m/s, the spreading time scale becomes approximately equal to the magnitude of the solidification time scale. In such a case, solidification affects the spreading process to a degree, such as slowing the spreading process and reducing the maximum extent of spreading.[12] Liu et al. reported that solidification causes a separation of the splat edge which could lead to formation of voids in the splat fringe region.[16] This is one mechanism for micropore formation during spraying of the coating. It will be considered herein when the solidification restricts the spreading.

Assuming that solidification initiates at the first contact region of the particle upon reaching the substrate (near the center region of the spreading particle), the solidification effect can be neglected during spreading when the thickness of the solidified layer, l_t, is much less than the final splat thickness, S_t, i.e., for $l_t/S_t << 1$. Regarding the initial contact area, A_p, as the area of a circle of particle diameter, d_p, a thermal energy balance for such an area gives

$$\rho H_p A_p l_t = (q_{sub} - q_{conv}) A_p t_{sp} \quad \text{(Eq 20)}$$

where q_{sub} and q_{conv} are heat transfer rates per unit area through the substrate and from plasma gas, respectively. Substitution of t_{sp} from Eq 13 into Eq 20 gives

$$t_{sp} = \frac{2}{3} \xi^2 \frac{S_t}{u_{p,i}} \text{ or}$$

$$\frac{l_t}{s_t} = \frac{3}{2} \frac{q_{sub} - q_{conv}}{\rho H_p u_{p,i}} \xi^2 \quad \text{(Eq 21)}$$

Therefore the solidification effect on the spreading process can be neglected for $l_t/S_t << 1$, that is

$$\frac{3}{2} \frac{q_{sub} - q_{conv}}{\rho H_p u_{p,i}} \xi^2 << 1 \quad \text{(Eq 22)}$$

For a fully molten particle, this condition can be written as

$$\frac{3}{2} \frac{h_s(T_m - T_s) - h_g(T_g - T_m)_i}{\rho H_{sf} u_{p,i}} \xi^2 << 1 \quad \text{(Eq 23)}$$

In terms of l_t/d_p, this condition becomes

$$\frac{l_t}{d_p} = \frac{l_t}{s_t} \frac{3}{2} \xi^{-2} = \frac{3}{2} \frac{h_s(T_m - T_s) - h_g(T_g - T_m)_i}{\rho H_{sf} u_{p,i}} \xi^2 << 1 \quad \text{(Eq 24)}$$

Bhola and Chandra,[21] on the basis of experimental results, estimated that for

$$\frac{l_t}{d_p} > 8 \times 10^{-3} \quad \text{(Eq 25)}$$

solidification would restrict the particle spreading. The coupling between the droplet solidification and the droplet spreading is simply being ignored herein. This may affect the utility of the analysis to a limited extent.

2.3.2 Prediction of Solidification. If the solidification does not affect the spreading process, the nature of solidification of a single splat depends on the relative magnitude of the solidification time scale and subsequent particle arrival time scale.

(i) $t_{fr} < t_{sa}$

When the solidification time scale, t_{fr} is less than the subsequent particle arriving time scale, t_{sa}, the spreading and solidification of each particle is completed before the next particle arrives. Then the intersplat boundaries are well defined. The porosity in the deposit would be relatively high due to the intersplat interstice.

(ii) $t_{fr} \sim t_{sa}$

When both time scales are comparable, thin liquid layers may remain on top of the solidifying splat when the subsequent particle impinges on it. This would reduce the porosity in the deposit.

(iii) $t_{fr} > t_{sa}$

When the solidification time scale is larger than the subsequent particle arriving time scale, the splat is primarily in the molten state when the next particle arrives. This condition eventually would lead to a thick liquid layer or liquid pool in a growing deposit, which may spill over the surface. The advantage of thermal plasma spraying may be lost and this condition should thus be avoided.

From the point of view of a single splat mentioned above, the desirable condition for the merit of thermal plasma spraying is

$$t_{fr} \leq t_{sa} \quad \text{(Eq 26)}$$

However, as the number of splats increases with time, because of the internal conduction resistance within the growing deposit, the solidification rate of a newly formed splat on the existing deposit is reduced, and eventually the time is reached when the liquid layer starts to form, even for $t_{fr} \leq t_{sa}$. The time when this would happen can be estimated by considering the internal conduction resistance within the growing deposit as described in the following section.

2.4. Multisplat Prediction

At some instant in time, t, the internal conduction resistance in a growing deposit, R_{cond}, can be represented as

$$R_{cond} = \frac{H}{kA_\xi} \quad \text{(Eq 27)}$$

where H is the thickness of an existing deposit and k is the thermal conductivity of deposit material. The deposit thickness, H, can be represented as

$$H = \left[\frac{t}{t_{sa}}\right] S_t = nS_i \quad \text{(Eq 28)}$$

where n is the integer number of t/t_{sa}, related to the particle arriving is a discrete event. Then the heat extraction rate, $\dot{Q}_{sub}$ from newly formed splat at time t to substrate can be given as

$$\dot{Q}_{sub} = \left[\frac{1}{\frac{nS_i}{k} + \frac{1}{h_s}}\right] A_\xi \overline{(T_p - T_s)} \quad \text{(Eq 29)}$$

Note that when

$$\frac{nS_i}{k} << \frac{1}{h_s} \quad \text{(Eq 30a)}$$

$$\text{or} \quad t << \frac{k}{h_s S_t} t_{sa} = Bi_s^{-1} t_{sa} \quad \text{(Eq 30b)}$$

(where Bi_s is the Biot number defined as $Bi_s = h_s S_t/k$) Eq 29 reduces to that of a single splat, as in Eq 18. This means that for a very short time duration defined by Eq 30b, the internal conduction resistance is negligible and a single splat analysis is valid.

Because the increased thermal resistance, $\dot{Q}_{sub}$ decreases and this, in turn, increases the solidification time of the newly formed splat. In turn, because of this increase in the mean time, the freezing time scale becomes comparable to the subsequent particle arriving time scale and the liquid layer then starts to form on top of the newly formed splat until the next particle arrives. Using Eq 16 and 29, and equating freezing time scale with subsequent particle arriving time scale yields

$$t_{fr} = t_{sa} \quad \text{(Eq 31)}$$

The time at which the liquid layer starts to form, t_l, can be estimated as

$$t_l = \frac{k}{S_t}\left\{\left|\frac{\frac{H_p}{t_{sa}} + \dot{Q}_{conv}}{A_\xi (T_p - T_s)}\right|^{-1} - \frac{1}{h_s}\right\} t_{sa} \quad \text{(Eq 32)}$$

When t_{sa} from Eq 15 is substituted into Eq 32, t_l is represented in terms of operating parameters. On the basis of this time scale, t_l, it is expected that for total spraying time, t_{ts}

(i) $t_{ts} < t_l$: deposit forms from fully solidified splats (Eq 33)

(ii) $t_{ts} \geq t_l$: thin liquid layer may form during solidification (Eq 34)

(iii) $t_{ts} >> t_l$: thick liquid layer forms on the growing deposit (Eq 35)

It is worth noting from Eq 32 that the convection effect from hot plasma gas can be neglected when

$$\frac{H_p}{t_{sa}} >> \dot{Q}_{conv} \quad \text{(Eq 36a)}$$

or

$$H_p >> \dot{Q}_{conv} \times t_{sa} \quad \text{(Eq 36b)}$$

This situation may occur when the latent heat of solidification is very large or t_{sa} is very small, as in the case of very large particle mass flow rate or very small particle diameter.

3. Discussion: Applicability to an Actual Process

The present analysis can be used in actual thermal plasma spray processes. To see its applicability, suppose that the particle size, d_p, and coating thickness, H, is specified.

3.1 Particle State at Impact

With available property data such as p, c, k, h, H_{sf}, T_m, T_{evp}, V, A_s, and information regarding operating parameters such as T_{go}, T_{po}, T_g, T_p, and $u_{p,i}$, the particle state at the moment of impingement on the substrate can be predicted or controlled. Main controlling parameters are the substrate distance, L, the particle velocity, u_p, and the plasma temperature, T_g. Controlling the substrate distance is straightforward, but has some restrictions, as mentioned below. Controlling the particle velocity may be achieved by varying the particle size and plasma gas velocity, i.e., volumetric flow rate. Of course, the former is usually specified.

3.2. Production of Fine Quality Coating with Preferred Structure

For fine quality coating from the thermal plasma spraying, the single splat criterion, Eq 26, should first be satisfied. This condition gives some restrictions on the particle mass flow rate and the spraying distance for a specified particle size. For a specified coating thickness, H, from Eq 28, the total solidification time, t_{ts}, is estimated in terms of the ratio, $(t_{ts}/t_{sa}) = (H/S_t)$, where S_t is estimated from the available spreading model as $S_t = (2/3)(d_p/\xi^2)$. Depending on the preferred porosity level, either Eq 33 or 34 needs to be satisfied. When a relatively high porosity coating is required (as in thermal barrier coatings), Eq 33 becomes the applicable criterion, whereas Eq 34 needs to be satisfied for production of a low porosity. For a specified coating thickness, H, $(H/S_t) >> 1$ and the total solidification time scale, $t_s = (H/S_t)t_{sa} >> t_{sa}$. Because the time scale, t_l, is related to t_{sa} through material properties, depending on the type of coating and material to be coated, either Eq 33 or 34 may not be satisfied. For metallic coatings, usually $t_l >> t_{sa}$ from Eq 32, thus Eq 33 can be satisfied, whereas Eq 34 may not, unless H/S_t is a very large value, which means very large coating thickness. Even for a very thick coating, Eq 33 is satisfied for some time after the spray process begins until the time is reached for Eq 34 to be satisfied. This suggests that the initial coating structure may differ from the later coating structure.

For ceramic coatings, largely because of the low value of the

thermal conductivity, t_l is not much larger than t_{sa}, whereas $t_{ts} > t_{sa}$. Thus $t_{ts} > t_l$ and Eq 33 is not satisfied shortly after the spraying begins. Consider a numerical example for the case of a ceramic coating thickness, $H = 500$ μm. The splat thickness becomes $S_t = (2/3)(d_p/\xi^2) = 3.7$ μm for $\xi = 3$. The total solidification time for $H = 500$ μm is $t_{ts} = (500/3.7)t_{sa} = 135t_{sa}$. For $T_p = 2000$ K, $k = 2.4$ W/m · K, $\rho = 5700$ kg/m^3, $H_{sf} = 7 \times 10^5$ J/kg, $H_p = \rho V H_{sf} = 2.61 \times 10^{-4}$ J for a fully molten particle. The splat area is $A_\xi = (\pi/4)\xi^2 d_p^2 = 1.76 \times 10^{-8}$ m^2. If we assume $\overline{(T_p - T_s)} = 10^3$ K, and $h_s = 10^4$ W/m^{2}K, from Eq 32, $t_l = 48 \cdot t_{sa}$. Thus, Eq 33 fails to be satisfied after one-third of the total spray time elapses from the start of the spray process.

From Eq 32, it may be inferred that for high-porosity coatings, the ceramic particle should have high thermal conductivity and a low H_p value (i.e., low density and low latent heat) to satisfy Eq 33. One way of reducing the H_p value could be to have the ceramic particle reach the substrate as a partially molten state, i.e., with some value of solid fraction.

4. Conclusions

An attempt has been made using scaling analysis to predict, globally, the characteristics of the thermal plasma spraying process in terms of basic operating and thermophysical parameters. The modeling was performed with the recognition that detailed physical processes, such as partial melting of individual particles during their flight, resolidification or evaporation of particles prior to their reaching the substrate, detailed splat dynamics and surface chemistry effects, particle-to-particle coupling in terms of hydrodynamic and solidification phenomena, and other detailed phenomena, cannot be described with the general approach taken here.

Although the analysis is made based on a simplified model considering discrete particle events, the analysis yields meaningful correlations by which it is possible to estimate two important processes: (1) the state of the particle at the moment of impact on substrate, and (2) the nature of solidification processes. Through relevant correlations, the limitation or restriction is also seen in obtaining preferred coating product. The correlations can be used to optimize the spraying process.

References

1. J.H. Zaat: "A Quarter of a Century of Plasma Spraying," *Ann. Rev. Mater. Sci.*, 1983, *13*, pp. 9-42.
2. L. Pawlowski: *The Science and Engineering of Thermal Spray Coating*, John Wiley & Sons, New York, 1995
3. Y. Zhou, Y. Wu, and E.J. Lavernia: "Process Modeling in Spray Deposition: A Review," *Int. J. Non-Equilibrium Processing*, 1997, *10*, pp. 95-183.
4. P. Eichert, C. Coddet, and M. Imbert: "On the Modeling Approach of DC Arc Plasma Flows by Implementation of the CFD Phoenics Code" in *Thermal Spray: Practical Solutions for Engineering Problems*, C.C. Berndt, ed., ASM International, Materials Park, OH, 1996, pp. 563-68.
5. S.V. Joshi: "Comparison of Particle Heat-Up and Acceleration During Plasma and High Velocity Oxy-Fuel Spraying," *Powder Metall. Int.*, 1992, *6*, pp. 373-80.
6. N. El-Kaddah, J. Mckelliget, and J. Szekely: "Heat Transfer and Fluid Flow in Plasma Spraying," *Metall. Trans. B*, 1984, *15B*, p. 59-67.
7. M. Vardelle, A. Vardelle, P. Fauchais, and M.I. Boulos: "Plasma-Particle Momentum and Heat Transfer: Modelling and Measurements," *AIChE J.*, 1983, *29*, pp. 236-43.
8. D.K. Das and R. Sivakumar: "Modelling of the Temperature and the Velocity of Ceramic Powder Particles in a Plasma Flame—I. Alumina," *Acta Metal. Mater.*, 1990, *38*, pp. 2187-92.
9. D.K. Das and R. Sivakumar: "Modelling of the Temperature and the Velocity of Ceramic Powder Particles in a Plasma Flame—II. Zirconia," *Acta Metal. Mater.*, 1990, *38*, pp. 2193-98.
10. J. Madejski: "Solidification of Droplets on a Cold Surface," *Int. J. Heat Mass Transfer*, 1976, *19*, pp. 1009-13.
11. H. Fukanuma and A. Ohmori: "Behavior of Molten Droplets Impinging on Flat Surfaces" in *Thermal Spray Industrial Applications*, C.C. Berndt and S. Sampath, ed., ASM International, Materials Park, OH, 1994, pp. 563-68.
12. M. Pasandideh-Fard and J. Mostaghimi: "Deformation and Solidification of Molten Particles on a Substrate in Thermal Plasma Spraying" in *Thermal Spray Industrial Applications*, C.C. Berndt and S. Sampath, ed., ASM International, Materials Park, OH, 1994, pp. 405-14.
13. T. Bennett and D. Poulikakos: "Splat-Quench Solidification: Estimating the Maximum Spreading of a Droplet in Spraying Processes," *J. Mater. Sci.*, 1993, *28*, pp. 963-70.
14. G. Trapaga and J. Szekely: "Mathematical Modeling of the Isothermal Impingement of Liquid Droplets in Spraying Process," *Metall. Trans. B*, 1991, *22B*, pp. 901-14.
15. H. Fukanuma: "A Porosity Formation and Flattening Model of an Impinging Molten Particle in Thermal Spray Coating," *J. Therm. Spray Technol.*, 1994, *3*, pp. 33-44.
16. H. Liu, E.J. Lavernia, and R.H. Rangel: "Numerical Simulation of Substrate Impact and Freezing of Droplets in Plasma Spray Process," *J. Phys. D: Appl. Phys.*, 1993, *26*, pp. 1900-08.
17. C. San Marchi, H. Liu, E.J. Lavernia, R.H. Rangel, A. Sickinger, and E. Muehlbergers: "Numerical Analysis of the Deformation and Solidification of a Single Droplet Impinging Onto a Flat Substrate," *J. Mater. Sci.*, 1993, *28*, pp. 3313-21.
18. F.M. White: *Viscous Fluid Flow*, 2nd ed., McGraw-Hill, New York, 1991.
19. I. Ahmed and T.L. Bergman: "Thermal Modeling of Plasma Spray Deposition of Nanostructured Ceramics," *J. Therm. Spray Technol.*, 1999, *8*, pp. 315-22.
20. M.C. Fleming: *Solidification Processing*, McGraw-Hill, New York, 1974.
21. R. Bhola and S. Chandra: "Splat Solidification of Tin Drops" in *Thermal Spray: Practical Solutions for Engineering Problems*, C.C. Berndt, ed., ASM International, Materials Park, OH, 1996, pp. 657-63.